

How do closed-compact multi-lamellar droplets form under shear flow? A possible mechanism

L. COURBIN¹, R. PONS^{1,2}, J. ROUCH¹ and P. PANIZZA^{1(*)}

¹ *Centre de Physique Moléculaire Optique et Hertzienne, UMR 5798*

Université Bordeaux I - 351 Cours de la Libération, 33400 Talence, France

² *Departament de Tecnologia de Tensioactius, CID/CSIC*

Jordi Girona 18-26, 08034 Barcelona, Spain

(received 5 August 2002; accepted in final form 28 October 2002)

PACS. 83.60.Rs – Shear rate-dependent structure (shear thinning and shear thickening).

PACS. 82.70.-y – Disperse systems; complex fluids.

PACS. 61.30.Eb – Experimental determinations of smectic, nematic, cholesteric, and other structures.

Abstract. – The formation of closed-compact multi-lamellar droplets obtained upon shearing both a lamellar phase (L_α) and a two-phase-separated lamellar-sponge (L_α - L_3) mixture is investigated as a function of the shear rate $\dot{\gamma}$, using small-angle light scattering (SALS) and cross-polarized optical microscopy. In both systems the formation of droplets occurs homogeneously in the cell at a well-defined wave vector $q_e \propto \dot{\gamma}^{1/3}$ via a *strain-controlled* process. These results suggest that the formation of droplets may be monitored in both systems by a buckling instability of the lamellae as predicted from a recent theory.

Introduction. – Large effort has been devoted to characterize the effect of shear flow on lyotropic lamellar (L_α) phases [1–4], and in particular to elucidate the mechanism of the formation of multi-lamellar droplets (MLVs, referred to in the literature as the “onion texture”), obtained upon shearing such phases [5–8]. A few years ago, inspired by the work of Ostwald *et al.* on smectic-A phases [9,10], Diat and Roux have conjectured that the transition to onions is triggered by a buckling (or undulation) instability [3]. According to them, this instability occurs because the gap spacing cell is not uniform in the experiment. At rest (*i.e.* without any shear flow), the existence of dislocations accommodates the spatial variation in the gap cell by permitting a change in the number of layers. At low shear rates, these dislocations can move with the mean flow whereas at higher shear rates they cannot follow it. This is believed to give rise to an effective dilative strain perpendicular to the layer, leading first to a buckling instability, likely followed by a secondary process leading to onion formation. A theory along these lines has been put forth a few years ago [11]. More recently, based on the coupling between the thermal undulations of the membrane and the flow, another buckling scenario which exists even at uniform gap spacing has been suggested by Zilman and Granek [12]. According to these authors, the suppression by the flow of the short-wavelength membrane undulations generates an effective lateral pressure leading to a buckling instability similar to that obtained

(*) E-mail: ppanizza@cribx1.u-bordeaux.fr

by dilative strain. The instability threshold predicted by this theory is in good agreement with experimental data provided that the viscosity of solvent is replaced by that of the L_α phase. Because of its resistance to the flow, the buckling pattern, once it has developed, is believed to become unstable in its turn. The lamellae are likely rolling up to form vesicles (onions) which can flow more easily. Bergenholtz and Wagner [5] and Zipfel *et al.* [6] have shown that the formation of onions in a Couette cell is strain-controlled, but they have not identified the exact nature of this mechanism. On the other hand, Léon *et al.* conclude that the shear-induced gelation they observed in a very dilute lamellar system occurs in a cone-plate cell via a nucleation process [7], a result which seems in contradiction with theoretical expectations [3,11,12]. Very recently, on a quaternary lamellar system stabilized by undulation interactions, we have shown that the formation of onions occurs homogeneously in the cell at a well-defined wave vector q_e via a *strain-controlled process*. A systematic study of q_e with experimental parameters [13] has revealed striking similarities with the most unstable wave vector of the buckling instability [12]: $q_B = a(\frac{d\eta}{D\kappa})^{1/3}\dot{\gamma}^{1/3}$, where d is the smectic distance, D the gap spacing, κ the bending modulus, η the viscosity, $\dot{\gamma}$ the shear rate, and a is a numerical constant.

The aim of this paper is to investigate and compare the mechanism of formation of closed-compact multi-lamellar droplets in lamellar phases (L_α) and in the L_α -rich region of phase-separated lamellar-sponge (L_α - L_3) mixtures made of AOT and brine. Let us emphasize that the size selection of the droplets is very different in the two cases. In L_α phases, it is governed by a balance between elastic and viscous stresses, whereas in (L_α - L_3) mixtures it results from a balance between surface tension and viscous stress (so-called Taylor's droplets) [14]. Besides, the droplet volume fraction in (L_α - L_3) phase-separated mixtures is not always 100% as for lamellar systems, but is fixed by the L_α volume fraction.

Experimental system. – We study a pseudobinary mixture made of sodium bis(2-ethylhexyl) sulfosuccinate (AOT) and brine (sodium chloride). Gosh and Miller have already published in detail the whole equilibrium phase diagram of this system [15]. At 25 °C, for low salinities ($S = 14$ g/l), flat bilayers stack upon each other and a lamellar phase (L_α) is observed. At high salinities ($S > 20$ g/l), the bilayers interconnect randomly and form a Newtonian bi-continuous phase referred to in the literature as sponge phase (or L_3 phase) [16]. For intermediate salinities, coexistence between L_α and L_3 phases is found. The effect of shear flow has been widely studied in this system. In the L_α region of this system, it results in the formation of a closed-compact assembly of multi-lamellar vesicles referred to in the literature as the “onion texture” [1,5,8,13]. These vesicles are mono-disperse and their size, which likely results from a balance between elastic and viscous stresses, varies as $\dot{\gamma}^{-1/2}$ [3,5,14]. Multi-lamellar droplets can also be prepared by shearing the two (L_α - L_3) phase-separated system in its L_α -rich region [14]. In this two-phase region, the droplet volume fraction is fixed by the volume fraction of the (L_α) phase and is not always 100% as for the “onion texture”. Very surprisingly, above close packing, the size R of these monodisperse droplets varies according to Taylor's prediction made for dilute emulsions [17]: $R \approx \sigma/\eta\dot{\gamma}$ (where σ and η are, respectively, the surface tension and the shear viscosity).

SALS scattering experiments under shear flow are performed in the velocity/vorticity plane (\vec{V}, \vec{Z}) with a home-made transparent Couette cell, that has been previously described [14]. Briefly, a circularly polarized He-Ne laser beam (wavelength is $\lambda = 632.8$ nm in vacuum) passes through the cell along the shear gradient direction and probes the sample in only one of the gaps.

Lamellar phase. – To investigate the formation of MLVs in the L_α phase region of the system, we prepared a solution made of 20% wt. AOT (99% purity from Fluka) and 80% wt. brine

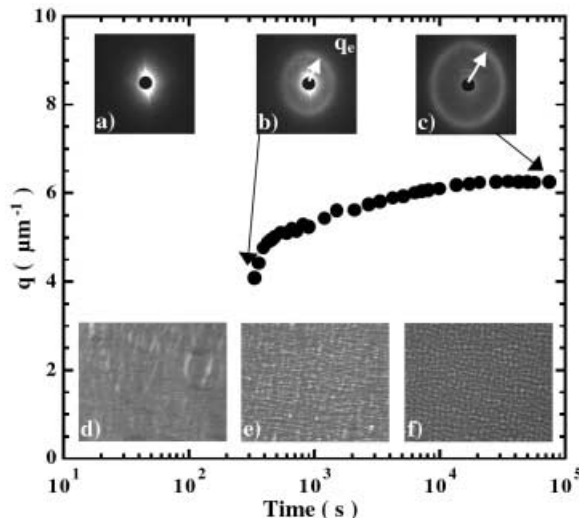


Fig. 1 – Variation of the position of the Bragg peak, q , as a function of time observed in SALS after a shear rate of $\dot{\gamma} = 15 \text{ s}^{-1}$ has been applied to a lamellar phase made of 20% wt. AOT and 80% wt. brine ($S = 14 \text{ g/l}$). Insets: SALS patterns observed on the screen in the (\vec{V}, \vec{Z}) -plane and cross-polarized microscopy images: (a, d) $t = 100 \text{ s}$, (b, e) $t = t_e = 550 \text{ s}$, and (c, f) $t = 56500 \text{ s}$ after the steady state is reached; the origin of time is taken once the shear is applied.

($S = 14 \text{ g/l}$). Once prepared, this phase is left at rest for a month to ensure thermodynamic equilibrium. It is then introduced into the Couette cell and sheared at a constant shear rate $\dot{\gamma}$, in order to form the MLVs. Figure 1 shows the evolution of the SALS pattern observed after $\dot{\gamma}$ is applied. We first observe an enhancement of the SALS pattern at small angles, slightly elongated in the vorticity direction, and after a well-defined time delay, t_e , the sudden emergence at a finite wave vector $q = q_e$ of a scattering ring (fig. 1b). When the shear rate is stopped, this ring persists with same q for a few hours, indicating that the micrometric shear-induced structure is meta-stable. Using this property, a few drops of the sample can be removed from the Couette cell and placed between two glass slides for optical-microscopy visualization. Observations made between crossed polarizers at t_e reveal a homogeneous modulation of the optical index in the whole cell (fig. 1e), corresponding to an onion texture. Upon a further shearing, the scattering ring moves towards larger wave vectors until it reaches its final position, $q = q_f \propto \dot{\gamma}^{1/2}$, characteristic of the steady-state onion structure (figs. 1c, f), indicating that the initial MLVs peel off until a mechanical balance is reached. When the flow is stopped before t_e , the texture is very similar to the one observed prior to shearing, namely no disperse vesicles are visible (fig. 1d). In agreement with our previous observations on the quaternary system [13], we find that $q_e \propto \dot{\gamma}^{1/3}$ and that the value of the strain at t_e , given by $\gamma_e = t_e \cdot \dot{\gamma}$, is a constant (fig. 2). These results show clearly that the formation of onions is a *strain-controlled* process occurring homogeneously in the cell at a well-defined wave vector q_e . The value of the critical strain necessary to form onion is large. Experimentally, one gets $\gamma_e \approx 5000$ which is similar to the value found for the quaternary system where $\gamma_e \approx 3500$ for $d \approx 100 \text{ \AA}$ [13]. Here also, the scaling $q_e \propto \dot{\gamma}^{1/3}$ is consistent with the prediction derived by Zilman and Granek for the most unstable wave vector of the buckling instability [12]. To check whether the order of magnitude of q_e is consistent with their prediction, *i.e.* $q_B = a \left(\frac{dn}{D\kappa} \right)^{1/3} \dot{\gamma}^{1/3}$, we used as numerical values for $d \approx 120 \text{ \AA}$, $D = 1 \text{ nm}$, $\eta \approx 10 \text{ Pa s}$, $\kappa \approx 3k_B T$ [18] and $a = 2.6$ and compare the numerical

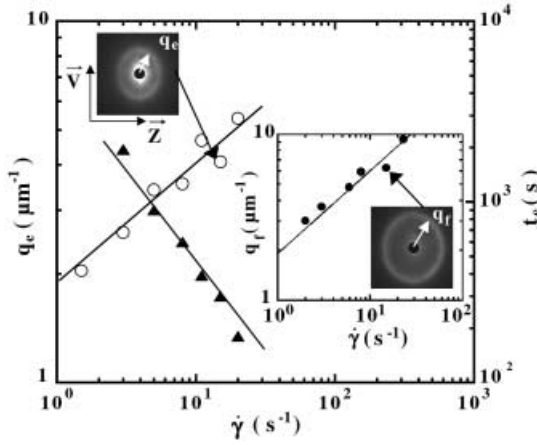


Fig. 2 – Variation of the position of the initial Bragg peak, q_e (\circ) and the time delay, t_e (\blacktriangle) observed in SALS as a function of the applied shear rate. Inset: shown is q_f (\bullet) as a function of $\dot{\gamma}$. The solid lines correspond to the best power law fits: $q_e \propto \dot{\gamma}^{1/3}$, $t_e \propto \dot{\gamma}^{-1}$ and $q_f \propto \dot{\gamma}^{1/2}$. The system is identical to that of fig. 1.

value of $s = a(\frac{dn}{D\kappa})^{1/3}$ with the slope of the curve q_e vs. $(\dot{\gamma})^{1/3}$ depicted in fig. 2. The values of s derived from the theory ($s \approx 0.6 \mu\text{m s}^{-1/3}$) and from the slope of the curve ($s \approx 1.9 \mu\text{m s}^{-1/3}$) are of the same order of magnitude. These results suggest therefore that the mechanism of onion formation in lamellar phases is universal and triggered by the buckling instability.

Lamellar and sponge phase coexistence region. – We prepare solutions in the two-phase (L_α - L_3) region with 20% wt. AOT and 80% wt. brine ($S = 16 \text{ g/l}$) corresponding to $\phi_{L_\alpha} = 82\%$ (where ϕ_{L_α} is the volume fraction of the L_α phase) at $T = 25^\circ\text{C}$. After leaving the solutions at rest for a few weeks, a macroscopic interface between the two phases is observed and its position in the cell allows us to determine ϕ_{L_α} . To study the effect of shear flow on this two-phase fluid, we first stir it gently in order to obtain a macroscopic homogeneous mixture. Then, we pour the mixture into the transparent cell and shear it at a constant $\dot{\gamma}$. For this system, we have already shown the existence of two steady states under shear flow. At low shear rates, we observed a glassy assembly made of mono-disperse multi-lamellar droplets immersed in the L_3 matrix whose size $R \propto 1/\dot{\gamma}$ is controlled by surface tension (Taylor's droplets [14]). Above a critical shear rate, $\dot{\gamma}_c = 18 \text{ s}^{-1}$, a transition to a colloidal mono-crystal (evidenced by the emergence of six Bragg peaks in the SALS pattern) occurs, leading to a different scaling $R \approx \dot{\gamma}^{-1/3}$ [14]. Figure 3 shows the evolution of the SALS pattern after the shear flow has been applied. As for the L_α system, we first observe an anisotropic enhancement of the scattered intensity at small angles. After a time delay t_e , a ring also emerges suddenly at $q = q_e$ (fig. 3b) and persists with same radius for a few tens of minutes if $\dot{\gamma}$ is stopped. At t_e , a homogeneous modulation of the optical index (fig. 3f), similar to that of an onion texture, can be observed under optical microscope. The variations of $q_e = \pi/R_e$ and of t_e with $\dot{\gamma}$ are identical to what we observe for the L_α system (fig. 4), namely: $t_e \propto 1/\dot{\gamma}$ and $q_e \propto \dot{\gamma}^{1/3}$. These observations indicate that the *strain-controlled* process at the origin of the formation of MLVs in L_α phases takes also likely place in the lamellar domains of the two-phase mixture upon shearing. Although the two systems we studied are very different, let us emphasize that the formation of MLVs seems in both case well described by the buckling scenario of Zilman and Granek. This result may suggest a possible universality of the phenomenon.

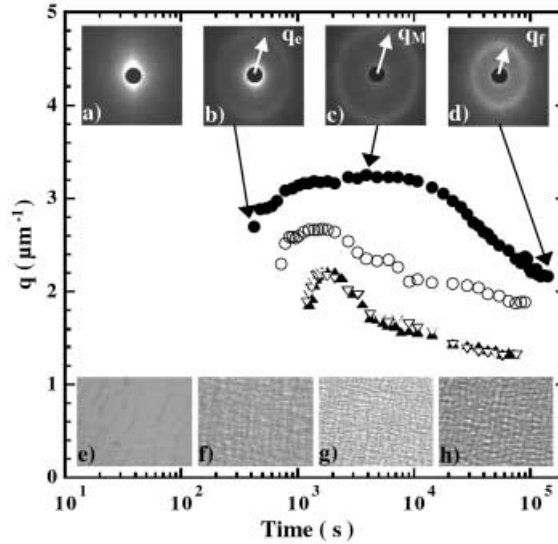


Fig. 3 – Variation of the size of the Bragg peak q with time after applying different shear rates to the premixed L_α/L_3 mixture ($S = 16 \text{ g/l}$): $\dot{\gamma} = 5 \text{ s}^{-1}$ (\blacktriangle) and (∇), $\dot{\gamma} = 8 \text{ s}^{-1}$ (\circ), and $\dot{\gamma} = 12 \text{ s}^{-1}$ (\bullet). Insets: SALS patterns observed in the (\vec{V}, \vec{Z}) -plane at different time t and corresponding images obtained between crossed polarizers: (a, e) $t = 90 \text{ s}$, (b, f) $t = t_e = 450 \text{ s}$, (c, g) $t = 3900 \text{ s}$ and (d, h) $t = 115200 \text{ s}$; the origin of time is taken once the shear is applied.

As for the L_α system, the initial radius of the MLVs in the L_α domains of the L_α - L_3 mixture, which is fixed by $R_e = \pi/q_e$, does not satisfy a mechanical balance. Therefore, when the shear flow is pursued at $\dot{\gamma}$, the size of the droplets changes continuously in order to reach equilibrium. However, contrary to L_α systems, this process presents two steps (see fig. 3): first,

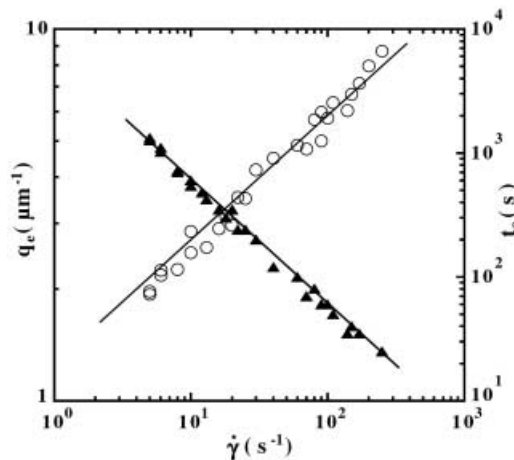


Fig. 4 – Variation of the emergence time, t_e (\blacktriangle) and the initial Bragg peak, q_e (Δ) as a function of $\dot{\gamma}$. The best power law fits give, respectively, $t_e \propto 6150/\dot{\gamma}$ and $q_e \propto \dot{\gamma}^{1/3}$. The system is the L_α/L_3 mixture ($S = 16 \text{ g/l}$).

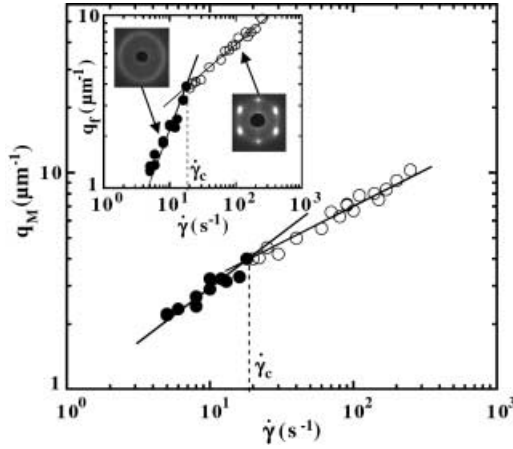


Fig. 5 – Variation of q_M and q_f (see inset) with the applied shear rate. The symbols \circ and \bullet represent, respectively, data for $\dot{\gamma} \geq \dot{\gamma}_c$ and for $\dot{\gamma} \leq \dot{\gamma}_c$. The system is identical to that of figs. 3 and 4.

the wave vector q characterizing the scattering ring increases to a pseudo-steady-state value q_M and then it decreases until it reaches its final size, q_f , corresponding to the closed-compact Taylor's droplets steady state. In agreement with our previous results [14], we observe that q_f varies as $\dot{\gamma}$ below $\dot{\gamma}_c$, and as $\dot{\gamma}^{1/3}$ above it (see inset of fig. 5), whereas q_M scales as $\dot{\gamma}^{1/2}$ below $\dot{\gamma}_c$, and as $\dot{\gamma}^{1/3}$ above it (fig. 5). Very surprisingly, for $\dot{\gamma} \leq \dot{\gamma}_c$ the variation of q_M with $\dot{\gamma}$ is identical to the scaling observed for the steady-state onion textures obtained upon shearing the L_α phases. This result suggests that once the initial MLVs are formed in the L_α domains, their size R decreases, as for L_α systems, until elastic and viscous stresses balance each other (*i.e.* $R_M = \pi/q_M \propto \dot{\gamma}^{-1/2}$). Within this picture, the surface tension between L_α and L_3 phases does not play a significant part and therefore, at this intermediate stage, the L_3 phase likely lies outside the L_α domains. Contrary to the behaviour observed in L_α phases, what can explain the further increase of the droplet size? Indeed, once the droplets have reached this intermediate stage, the L_3 phase must intercalate between these droplets since we know that for $\dot{\gamma} \leq \dot{\gamma}_c$, the steady-state droplets are immersed in the L_3 phase [14]. During this slow process, the surface tension adds up to the elastic force applied on the droplets. As a result, the droplet size increases continuously until a balance between surface tension (which overcomes elasticity) and viscous stress is reached: $R_f \approx \sigma/\eta\dot{\gamma}$ [14]. This scenario raises an important question. Namely, what is the origin of the pressure gradient triggering the L_3 phase between MLVs inside the L_α domains?

As a final comment, our results show that the mechanism of formation of closed-compact multi-lamellar droplets under shear flow in a Couette cell seems to be universal in both L_α phases and L_α/L_3 two-phase mixtures. This mechanism results from a strain-controlled process occurring homogeneously in the cell at a finite wave vector q_e . The variation of q_e with the parameters of the experiments suggests that the buckling instability controls the initial droplet size as expected by the theory.

It is a pleasure to thank T. DOUAR and M. WINCKERT for technical assistance. This work was supported by the Conseil Régional d'Aquitaine (CTP grant No. 980209202).

REFERENCES

- [1] RAMASWAMY S., *Phys. Rev. Lett.*, **69** (1992) 112.
- [2] BRUISMA R. and RABIN Y., *Phys. Rev. A*, **45** (1992) 994.
- [3] DIAT O., NALLET F. and ROUX D., *J. Phys. II*, **3** (1993) 1427.
- [4] YAMAMOTO J. and TANAKA H., *Phys. Rev. Lett.*, **74** (1995) 932.
- [5] BERGENHOLTZ J. and WAGNER N. J., *Langmuir*, **12** (1996) 3122.
- [6] PANIZZA P., COLIN A., COULON C. and ROUX D., *Eur. J. Phys. B*, **4** (1998) 65.
- [7] LÉON A., BONN D., MEUNIER J., AL-KAHWAJI A., GREFFIER O. and KELLAY H., *Phys. Rev. Lett.*, **84** (2000) 1335.
- [8] ZIPFEL J., NETTESHEIM F., LINDNER P., LE T. D., OLSSON U. and RICHTERING W., *Europhys. Lett.*, **53** (2001) 335.
- [9] OSTWALD P. and KLÉMAN M., *J. Phys. (Paris) Lett.*, **43** (1983) L-411.
- [10] OSTWALD P. and BEN-ABRAHAM S. I., *J. Phys. (Paris)*, **43** (1982) 1193.
- [11] WUNENBURGER A. S., COLIN A., COLIN T. and ROUX D., *Eur. Phys. J. E*, **2** (2000) 277.
- [12] ZILMAN A. G. and GRANEK R., *Eur. Phys. J. B*, **11** (1999) 593.
- [13] COURBIN L., ROUCH J., DELVILLE J. P. and PANIZZA P., *Phys. Rev. Lett.*, **89** (2002) 148305.
- [14] COURBIN L., CRISTOBAL G., ROUCH J. and PANIZZA P., *Europhys. Lett.*, **55** (2001) 880.
- [15] GOSH O. and MILLER C. A., *J. Phys. Chem.*, **91** (1987) 258.
- [16] See, for instance, PORTE G., in *Micelles, Membranes, Microemulsions and Monolayers*, edited by GELBART W. M., BEN-SHAUL A. and ROUX D. (Springer Verlag, New York) 1994.
- [17] TAYLOR G. I., *Proc. R. Soc. London, Ser. A*, **146** (1934) 501.
- [18] FREYSSINGEAS E., NALLET F. and ROUX D., *Langmuir*, **12** (1996) 6028.